Bo Wang
School of Mechanical and Aerospace Engineering, Oklahoma State University, Stillwater, OK 74078
e-mail: bobowang0406@gmail.com

Pravarsha Ghanta
School of Mechanical and Aerospace Engineering, Oklahoma State University, Stillwater, OK 74078
e-mail: pravars@okstate.edu

Sandra Vinnikova
School of Mechanical and Aerospace Engineering, Oklahoma State University, Stillwater, OK 74078
e-mail: s.vinnikova@icloud.com

Siyuan Bao
School of Civil Engineering, University of Science and Technology of Suzhou, Suzhou 215011, China;
School of Mechanical and Aerospace Engineering, Oklahoma State University, Stillwater, OK 74078
e-mail: bsiyuan@mail.usts.edu.cn

Junfeng Liang
Department of Electrical Engineering, The University of Texas at Dallas, Richardson, TX 75080
e-mail: jxl150230@utdallas.edu

Hongbing Lu
Department of Electrical Engineering, The University of Texas at Dallas, Richardson, TX 75080
e-mail: hongbing.lu@utdallas.edu

Shuodao Wang[1]
School of Mechanical and Aerospace Engineering, Oklahoma State University, Stillwater, OK 74078
e-mail: shuodao.wang@okstate.edu

Wrinkling of Tympanic Membrane Under Unbalanced Pressure

Mechanics of tympanic membrane (TM) is crucial for investigating the acoustic transmission through the ear. In this study, we studied the wrinkling behavior of tympanic membrane when it is exposed to mismatched air pressure between the ambient and the middle ear. The Rayleigh–Ritz method is adopted to analyze the critical wrinkling pressure and the fundamental eigenmode. An approximate analytical solution is obtained and validated by finite element analysis (FEA). The model will be useful in future investigations on how the wrinkling deformation of the TM alters the acoustic transmission function of the ear. [DOI: 10.1115/1.4035858]

1 Introduction

Tympanic membrane (TM, commonly referred to as the ear drum) is a thin biomembrane that separates the auditory canal from the middle ear cavity (Fig. 1(*a*)). It plays an important role in hearing by transmitting acoustic waves into the cochlea. Under many environmental circumstances, ambient (external) air pressure can vary by a few Pa to a few kPa, which can result in significant influence on the hearing ability [1,2]. Therefore, it is crucially important to study the mechanical properties and material behavior of the TM. Liang et al. [3] combined experimental and numerical methods to measure the mechanical properties of guinea pig TM subjected to quasi-static pressure and estimated the Young's modulus of guinea pig TM from 15.2 to 28.3 MPa. From their FEA results, when the ambient pressure is lower than the pressure in the middle ear, the TM forms a multiple-wave wrinkling pattern in the out-of-plane direction [1,2]. The wrinkling deformation can be the source of significant change in the acoustic characteristics of the TM and therefore alters the hearing of the ear. However, the mechanism of this wrinkling is not very clear, which hinders further investigations on how the pressure mismatch alters acoustic characteristics. Although numerous studies investigated the buckling of plates, membranes, and shells [4–9], the analyses are not directly

[1]Corresponding author.
Manuscript received December 27, 2016; final manuscript received January 23, 2017; published online February 8, 2017. Editor: Yonggang Huang.

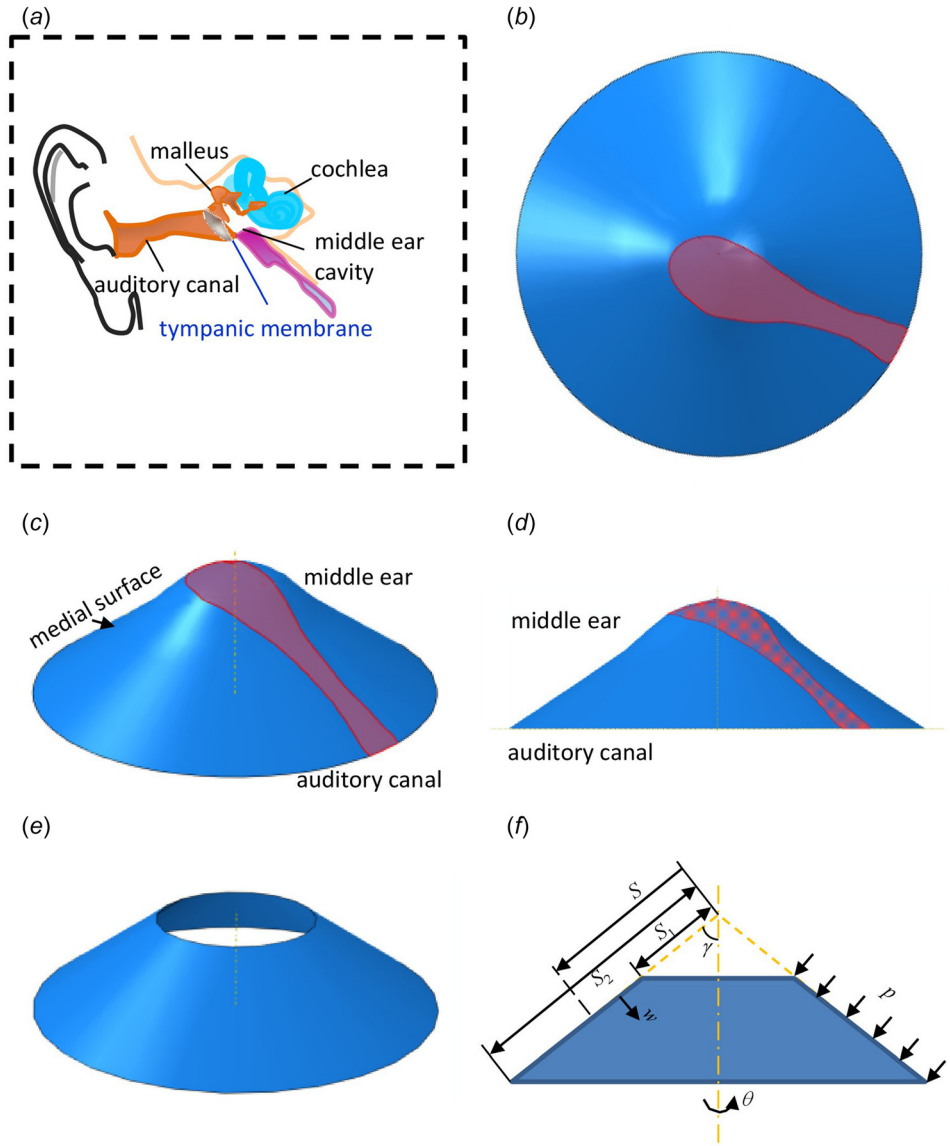

Fig. 1 Schematics of the tympanic membrane (TM) and the mechanics model: (*a*) location of the TM, (*b*) projection-view of the TM from the medial side, (*c*) 3D-view of the TM, (*d*) side-view of the TM, (*e*) 3D-view of the simplified axial-symmetric mechanics model, and (*f*) side-view of the mechanics model

applicable to the buckling of soft biomembranes here. For example, Sharghi et al. [4] used an analytical approach to investigate the buckling of truncated conical shells made of composite materials with general lamination sequence. Dung et al. [5] studied the buckling of an eccentrically stiffened sandwich truncated conical shell subjected to an axial compressive load and uniform pressure. Anh et al. [7] investigated the nonlinear stability of thin functionally graded material annular spherical shell on elastic foundations subjected to external pressure and thermal loads. Sofiyev and Kuruoglu [9] used the large deformation theory and von Karman–Donnell-type of kinematic nonlinearity to study the buckling of truncated conical composite shell surrounded by an elastic medium. Most of these studies focused on macroscopic structures with composite materials and are not readily applicable to soft biomembranes such as the TM here. In this study, based on the von Karman–Donnell type of kinematic and nonlinear shell theory, an analytical model is developed for the wrinkling of the TM. The results are validated by FEA, which will inform future studies on acoustic characteristics.

2 Mechanics Model

Figure 1(*c*) shows a schematic of the three-dimensional shape of the TM which resembles sand hill with the top of the hill pointing toward the middle ear cavity. The surface facing toward the middle ear is referred to as the medial side of the TM (Fig. 1(*c*)), and the opposite surface is called the lateral side. The outer rim of the TM is attached to the auditory canal, and the highlighted area (purple in Figs. 1(*b*)–1(*d*)) is firmly attached to the manubrium bone of the malleus. Figures 1(*b*) and 1(*d*) show the projection-view (along the axis direction, dashed line in Fig. 1(*c*)) and side-view of the TM, respectively. Typically, e.g., for guinea pig, the Young's modulus of the manubrium bone (~10 GPa) is 3 orders of magnitude larger than that of the TM (15.3–28 MPa); therefore, the TM is considered to be fixed in the area attached to the manubrium bone. We simplified the TM to be an axially symmetric truncated conical shell as shown in Fig. 1(*e*), which is fixed at the top rim to simulation the support from the manubrium bone and fixed at the bottom rim to simulation the support from the auditory

canal. The coordinates are shown in Fig. 1(*f*): S is the distance from the vertex along a generator; θ is the angle in the circumferential direction; u and v (not shown in the figures) denote the displacement along the S and θ directions, respectively, and w is the displacement perpendicular to the membrane surface (Fig. 1(*f*)). Geometric parameters of the truncated conical shell include γ—the semivertical angle, S_1 and S_2—the distances from the vertex to the top and bottom rims, respectively. When the ambient (external) pressure is lower than the pressure in the middle ear cavity (negative pressure), a uniform pressure p is applied on the medial side of the TM, acting against the surface normal (Fig. 1(*f*)).

When the conical shell deforms, we assume the following kinematically admissible displacement field which is adopted in previous stability analysis of conical shell [10]

$$\begin{cases} u = A\cos\left[\dfrac{\pi(S-S_1)}{S_2-S_1}\right]\cos(k\theta) \\ v = B\sin\left[\dfrac{\pi(S-S_1)}{S_2-S_1}\right]\sin(k\theta) \\ w = C\sin\left[\dfrac{\pi(S-S_1)}{S_2-S_1}\right]\cos(k\theta) \end{cases} \tag{1}$$

where A, B, and C are the buckling amplitudes to be determined, and k is wave number. This displacement field satisfies the boundary condition of $u=v=w=0$ at $S=S_1$ and at $S=S_2$ and also describes k wrinkling waves in a circumference.

The strain–displacement relations at the middle surface of a deformed truncated conical shell are given by [11]

$$\begin{cases} \varepsilon_S = \dfrac{\partial u}{\partial S} \\ \varepsilon_\theta = \dfrac{1}{S\sin\gamma}\dfrac{\partial v}{\partial\theta} + \dfrac{u}{S} - \dfrac{w}{S}\cot\gamma \\ \varepsilon_{S\theta} = \dfrac{1}{S\sin\gamma}\dfrac{\partial u}{\partial\theta} - \dfrac{v}{S} + \dfrac{\partial v}{\partial S} \end{cases} \tag{2}$$

in which the membrane strains are assumed to be small at the onset of wrinkling, and therefore only the leading-order terms are considered. The bending curvatures are [11]

$$\begin{cases} \chi_S = -\dfrac{\partial^2 w}{\partial S^2} \\ \chi_\theta = -\dfrac{1}{S}\dfrac{\partial w}{\partial S} - \dfrac{1}{S^2\sin^2\gamma}\dfrac{\partial^2 w}{\partial\theta^2} \\ \chi_{S\theta} = \dfrac{1}{S^2\sin\gamma}\dfrac{\partial w}{\partial\theta} - \dfrac{1}{S\sin\gamma}\dfrac{\partial^2 w}{\partial S\partial\theta} \end{cases} \tag{3}$$

where finite rotation of the shell is taken into account by considering the second-order terms.

The unbalanced pressure loading is considered to be quasi-static (as is in the corresponding experiments of Liang et al. [3]); therefore, the transient response of the TM due to viscoelasticity is not considered in this study. Experiments also found that the TM is linear elastic for strains up to ~10% [3]; therefore, material nonlinearity is not considered when analyzing the small deformation at initial wrinkling. However, for future studies on post-buckling of the TM under auditory high frequency range, a frequency-dependent viscoelastic–hyperelastic model should be taken into account. The strain energy of the structure consists of the membrane energy $U_{\rm m}$ and the bending energy $U_{\rm bend}$. The membrane and bending energies are given as [10]

$$U_{\rm m} = \frac{Eh}{2(1-\nu^2)}\int_0^{2\pi}\int_{S_1}^{S_2}\left(\varepsilon_S^2 + 2\nu\varepsilon_\theta\varepsilon_s + \varepsilon_\theta^2 + \frac{1-\nu}{2}\cdot\varepsilon_{S\theta}^2\right) \times (S\sin\gamma)\mathrm{d}S\mathrm{d}\theta \tag{4}$$

and

$$U_{\rm bend} = \frac{Eh^3}{24(1-\nu^2)}\int_0^{2\pi}\int_{S_1}^{S_2}\left(\chi_S^2 + 2\nu\chi_\theta\chi_s + \chi_\theta^2 + \frac{1-\nu}{2}\cdot\chi_{S\theta}^2\right) \times (S\sin\gamma)\mathrm{d}S\mathrm{d}\theta \tag{5}$$

where E and ν are the Young's modulus and Poisson's ratio of the membrane, respectively, and h is the thickness of the TM.

Following the approach developed by Baruch and Singer [11], Steyer and Zien [12] and Kendrick [13–15] for hydrostatically loaded conical shells, the work by the external load p is calculated as (see the Appendix for details) [11]

$$W_p = \frac{p}{2}\tan\gamma\int_0^{2\pi}\int_{S_1}^{S_2}\left[\frac{S^2\sin\gamma}{2}\left(\frac{\partial w}{\partial S}\right)^2 + \frac{1}{\sin\gamma}\left(\frac{\partial w}{\partial\theta}\right)^2\right]\mathrm{d}S\mathrm{d}\theta \tag{6}$$

The total potential energy of the system is obtained by

$$\Pi = U_{\rm m} + U_{\rm bend} - W_p \tag{7}$$

Minimizing the total potential energy Π with respect to the amplitudes A, B, and C, i.e.,

$$\begin{cases} \dfrac{\partial\Pi}{\partial A} = 0 \\ \dfrac{\partial\Pi}{\partial B} = 0 \\ \dfrac{\partial\Pi}{\partial C} = 0 \end{cases} \tag{8}$$

yields

$$\begin{bmatrix} e_{11} & e_{12} & e_{13} \\ e_{12} & e_{22} & e_{23} \\ e_{13} & e_{23} & e_{33} \end{bmatrix}\begin{bmatrix} A \\ B \\ C \end{bmatrix} = 0 \tag{9}$$

where e_{ij} (i, $j=1$, 2, 3) are analytical functions (given in the Appendix, $e_{ij}=e_{ji}$) depending on the nondimensional parameters γ, S_2/S_1, S_2/h, k, and p/E. Nonzero solution exists for Eq. (9) only when the determinant of the $[e_{ij}]$ matrix equals zero, i.e., $\det(e_{ij})=0$ which yields the critical pressure $p_{\rm cr}$ as

$$p_{\rm cr} = E\cdot f\left(\gamma, \frac{S_2}{S_1}, \frac{S_2}{h}, \nu, k\right) \tag{10}$$

where f is a nondimensional function determined from $\det(e_{ij})=0$. The wave number $k_{\rm min}$ corresponds to the lowest critical $p_{\rm cr\_min}$ can be obtained by solving

$$\frac{\partial p_{\rm cr}}{\partial k} = 0 \tag{11}$$

and then rounding to the nearest smaller/larger integer.

3 Results and Discussion

For the TM of the guinea pig [3], the Young's modulus is taken as $E=25$ MPa, the Poisson's ratio is $\nu=0.20$, and the thickness is $h=10\,\mu$m. The shape of a typical TM is characterized by

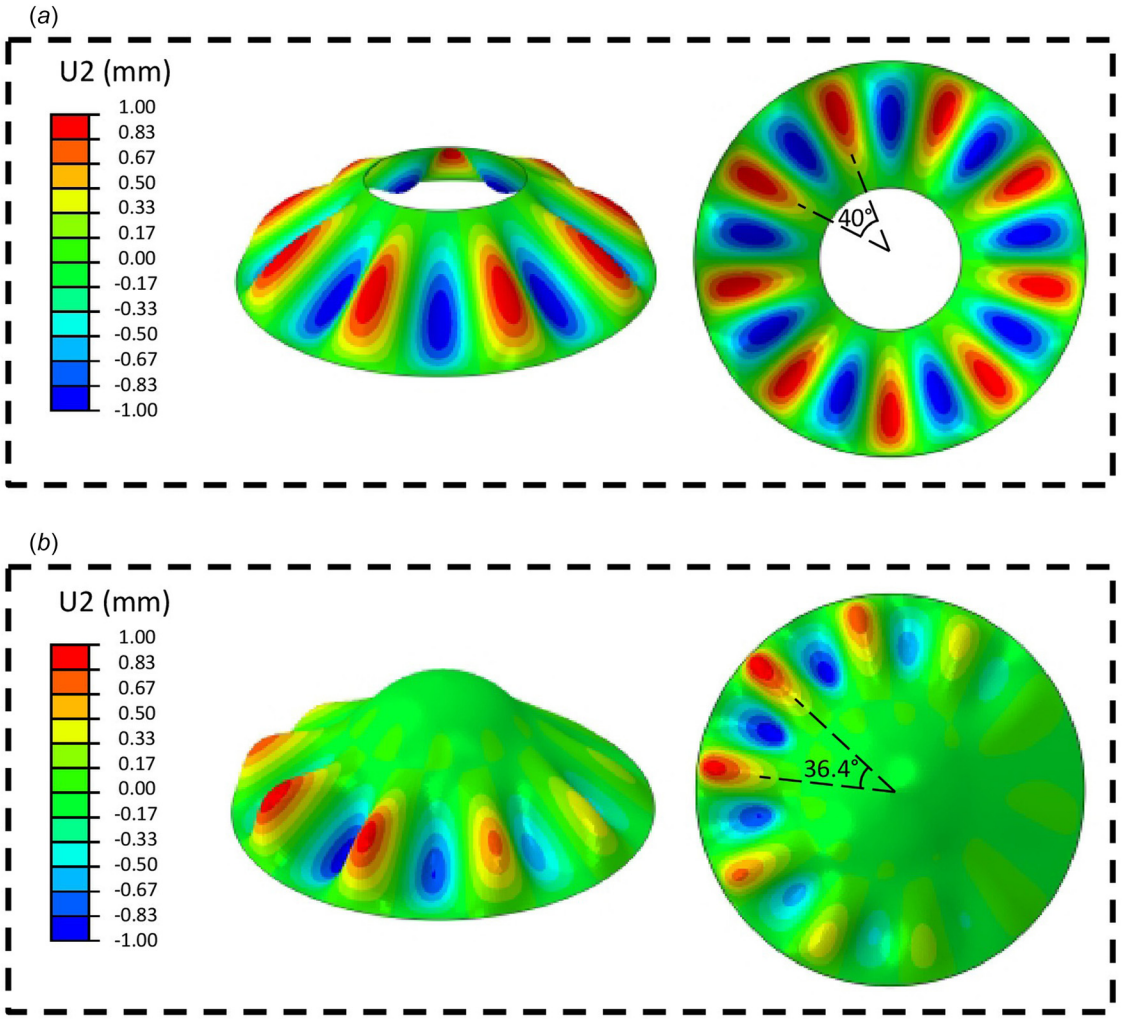

Fig. 2 Wrinkling patterns of the TM obtained by FEA using (*a*) the simplified axial-symmetric model in Fig. 1(*e*) and (*b*) TM supported by the manubrium bone as in Figs. 1(*b*)–1(*d*)

$\gamma = 55.4$ deg, $S_2 = 3.04$ mm, and $S_1 = 1.25$ mm. Using these parameters, Eq. (11) gives $k = 8.47$, then the p_{cr} at $k = 8$ and $k = 9$ are compared. It was found that $k = 9$ corresponds to the minimum $p_{cr} = 30.5$ Pa. These values agree very well with FEA (linear perturbation analysis with shell elements, based the above data, to extract the buckling deformation mode and the corresponding critical pressure) that yields $k = 9$ and $p_{cr} = 30.9$ Pa. The wrinkled shape from the FEA (Fig. 2(*a*)) also agrees reasonably well with experimental and post-buckling FEA images obtained by Liang et al. [3].

FEA was also used to validate the assumption of simplified axial-symmetric shape. Figure 2(*b*) shows an FEA model that accounts for the exact shape of the TM and the manubrium bone, which yields similar wrinkling pressure ($p_{cr} = 29.4$ Pa, comparable to the 30.5 Pa by the analytical model) and patterns (the period of the wrinkling waves is 36.4 deg, compared to 40 deg by the analytical model). These results confirm that the effect of the manubrium bone on the critical pressure and the wrinkling shape is relatively small.

For TMs of similar shape (keeping $\gamma = 55.4$ deg, $S_2/S_1 = 2.43$, and $\nu = 0.2$), a simplified expression for the critical pressure can be obtained by

$$\frac{p_{cr}}{E} \approx 10^{1/4} \cdot \left(\frac{h}{S_2}\right)^{5/2} \tag{12}$$

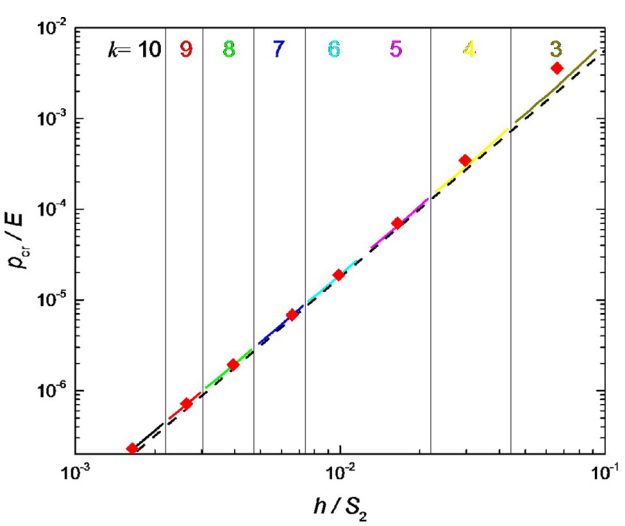

Fig. 3 Scaling law plotted as the normalized critical pressure versus normalized thickness. The solid lines correspond to the analytical solution for different wave number *k*, the dashed line corresponds to the approximate expression in Eq. (12), and the diamond dots correspond to FEA results.

which is a very useful scaling law for in vivo measurement of the mechanical properties of the TM [3]. Equation (12) is plotted in Fig. 3, which shows very nice agreements between the analytical model, the approximate expression, and FEA.

4 Conclusions

In this paper, an analytical model is established for the wrinkling of a soft biomembrane (the TM) undergoing mismatch pressure between the middle and external ear. The critical wrinkling pressure and the wave number are obtained analytically, which agree very well with FEA and experimental observations. It was found that the support from the manubrium bone has small effect on the critical wrinkling pressure and the wrinkling shape. The analytical model established here provides a useful tool for future studies on the mechanics of TM such as in vivo mechanical property measurements and effects of pressure on the acoustic transmission function of the eardrum.

Acknowledgment

S. Wang acknowledges the support from the ASME Applied Mechanics Division—Haythornthwaite Foundation Research Initiation Grant. H. Lu acknowledges Louis A. Beecherl Jr. Chair.

S. Wang acknowledges partial support from the National Natural Science Foundation of China (NSFC) (Nos. 11272260, 11172022, 11572022, 51075327, and 11302038). H. Lu acknowledges the support of Department of Defense of the United States (DOD) (W81XWH-13-MOMJPC5-IPPEHA, W81XWH-14-1-0228), National Institutes of Health (NIH) (R01DC011585), National Science Foundation (NSF) (CMMI-1636306, ECCS-1307997), and Air Force Office of Scientific Research (AFOSR) (FA9550-14-1-0227).

Appendix

A.1 Work Done by Hydrostatic Pressure. To calculate the work done by the external hydrostatic pressure, we start by calculating the prebuckling stress resultants via equilibrium under the reference (undeformed) geometry. Using the membrane equations [16] and consider only the pressure normal to the shell surface, one finds these prebuckling stress resultants to be

$$\begin{cases} N_S^0 = -\dfrac{PS}{2}\tan\gamma \\ N_\theta^0 = -PS\tan\gamma \\ N_{S\theta}^0 = 0 \end{cases} \tag{A1}$$

where N_S^0, N_θ^0, and $N_{S\theta}^0$ are the membrane stresses along the S, θ, and shear directions, respectively. Upon the onset of buckling, the work done by pressure p is equal to twice the strain energy in the shell, in which finite strain components of ε_S', ε_θ', and $\varepsilon_{S\theta}'$ need to be considered

$$\begin{cases} \varepsilon_S' = \dfrac{\partial u}{\partial S} + \dfrac{1}{2}\left(\dfrac{\partial w}{\partial S}\right)^2 \\ \varepsilon_\theta' = \dfrac{1}{S\sin\gamma}\dfrac{\partial v}{\partial\theta} + \dfrac{u}{S} - \dfrac{w}{S}\cot\gamma + \dfrac{1}{2S^2\sin^2\gamma}\left(\dfrac{\partial w}{\partial\theta}\right)^2 \end{cases} \tag{A2}$$

The work done by the external load is then obtained by

$$W_p = \int_0^{2\pi}\int_{S_1}^{S_2}\left(N_S^0\varepsilon_S' + N_\theta^0\varepsilon_\theta' + N_{S\theta}^0\varepsilon_{S\theta}'\right)S\sin(\gamma)\mathrm{d}S\mathrm{d}\theta \tag{A3}$$

By taking $N_{S\theta}^0 = 0$ and simplifying Eq. (A3) using the displacement field in Eq. (1), Eq. (6) can be obtained.

A.2 Energy minimization. The total potential energy Π is derived to be

$$\begin{aligned} \Pi = & \left[KA^2 + \frac{(1-\nu)KB^2}{2} + DC^2\left(\frac{\pi}{S_2-S_1}\right)^2\right]\frac{\pi\sin\gamma}{2}\left(\frac{\pi}{S_2-S_1}\right)^2\left(\frac{S_2^2-S_1^2}{4}\right) \\ & + \frac{1}{4}\pi KBAk(3b_2 - \pi - b_2\nu - \nu\pi) - \frac{A\cos\gamma\pi KC}{2}(b_2 - \nu\pi) \\ & + \left\{\begin{array}{l} +\dfrac{K\pi C^2\cos^2\gamma}{2\sin\gamma} - \pi KkCB\cot\gamma + \dfrac{\pi KA^2}{2\sin\gamma}\left[\sin^2\gamma + \dfrac{(1-\nu)k^2}{2}\right] \\ +\dfrac{\pi KB^2}{2\sin\gamma}\left[k^2 + \dfrac{(1-\nu)\sin^2\gamma}{2}\right] + \dfrac{\pi DC^2}{\sin\gamma}\left(\dfrac{\pi}{S_2-S_1}\right)^2\left(k^2 + \dfrac{\sin^2\gamma}{2}\right) \end{array}\right\}\frac{1}{2}\ln\left(\frac{S_2}{S_1}\right) \\ & - \frac{1}{2}b_1\left\{\begin{array}{l} \dfrac{\pi KB^2}{2\sin\gamma}\left[k^2 + \dfrac{(1-\nu)\sin^2\gamma}{2}\right] + \dfrac{K\pi C^2\cos^2\gamma}{2\sin\gamma} \\ -\dfrac{\pi KA^2}{2\sin\gamma}\left[\sin^2\gamma + \dfrac{(1-\nu)k^2}{2}\right] - \pi KCBk\cot\gamma \\ +\dfrac{\pi DC^2}{\sin\gamma}\left(\dfrac{\pi}{S_2-S_1}\right)^2\left[(2\nu-1)k^2 - \sin^2\gamma\right] \end{array}\right\} \\ & - \frac{1}{4}\frac{\pi Db_1C^2k^2}{\sin\gamma}\left(\frac{2\pi}{S_2-S_1}\right)^2\left[(2-\nu) - \frac{k^2}{2\sin^2\gamma}\right] \\ & - \frac{\pi p}{2}C^2\frac{\sin^2\gamma}{\cos\gamma}\left(\frac{\pi}{S_2-S_1}\right)^2\left[\frac{S_2^3-S_1^3}{12} + \frac{(S_2-S_1)^3}{8\pi^2}\right] - \frac{\pi pC^2k^2}{2\cos\gamma}\frac{S_2-S_1}{2} \end{aligned} \tag{A4}$$

where $b_1 = \int_{S_1}^{S_2} 1/S\cos[2\pi(S-S_1)/S_2-S_1]\mathrm{d}S$, $b_2 = \int_{S_1}^{S_2} 1/S\sin[2\pi(S-S_1)/S_2-S_1]\mathrm{d}S$, $K = Eh/(1-\nu^2)$, and $D = Kh^2/12$. Minimizing Π by Eq. (8) yields Eq. (9), and

$$e_{11} = \sin\gamma\left(\frac{\pi}{S_2/S_1-1}\right)^2\left(\frac{S_2^2/S_1^2-1}{4}\right) + \frac{1}{2\sin\gamma}\left[\sin^2\gamma+\frac{(1-\nu)k^2}{2}\right]\left[\ln\left(\frac{S_2}{S_1}\right)+b_1\right]$$

$$e_{12} = \frac{k(3b_2-\pi-b_2\nu-\nu\pi)}{4}$$

$$e_{13} = -\frac{\cos\gamma(b_2-\nu\pi)}{2}$$

$$e_{22} = \frac{(1-\nu)\sin\gamma}{2}\left(\frac{\pi}{S_2/S_1-1}\right)^2\left(\frac{S_2^2/S_1^2-1}{4}\right) + \frac{1}{2\sin\gamma}\left[k^2+\frac{(1-\nu)\sin^2\gamma}{2}\right]\left[\ln\left(\frac{S_2}{S_1}\right)-b_1\right]$$

$$e_{23} = -\frac{k\cot\gamma[\ln(S_2/S_1)-b_1]}{2}$$

and

$$e_{33} = \frac{\sin\gamma}{12}\frac{h^2}{S_1^2}\left(\frac{\pi}{S_2/S_1-1}\right)^4\left(\frac{S_2^2/S_1^2-1}{4}\right) + \frac{1}{2}\ln\left(\frac{S_2}{S_1}\right)\left[\frac{\cos^2\gamma}{\sin\gamma}+\frac{1}{6\sin\gamma}\frac{h^2}{S_1^2}\left(\frac{\pi}{S_2/S_1-1}\right)^2\left(k^2+\frac{\sin^2\gamma}{2}\right)\right] - \frac{b_1\cos^2\gamma}{2\sin\gamma} - \frac{b_1k^2}{6\sin\gamma}\frac{h^2}{S_1^2}\left(\frac{\pi}{S_2/S_1-1}\right)^2\left(2-\nu-\frac{k^2}{2\sin^2\gamma}\right) - \frac{1}{3\sin\gamma}\left(\frac{\pi}{S_2/S_1-1}\right)^2 b_1\frac{h^2}{S_1^2}\left[(2\nu-1)k^2-\sin^2\gamma\right] - \frac{(1-\nu^2)p\sin^2\gamma}{E\cos\gamma}\frac{S_1}{h}\left(\frac{\pi}{S_2/S_1-1}\right)^2 \times\left[\frac{S_2^3/S_1^3-1}{12}+\frac{(S_2/S_1-1)^3}{8\pi^2}\right] - \frac{(1-\nu^2)pk^2}{E\cos\gamma}\frac{S_1}{h}\frac{S_2/S_1-1}{2}$$

References

[1] Dirckx, J. J. J., and Decraemer, W. F., 1991, "Human Tympanic Membrane Deformation Under Static Pressure," Hear. Res., **51**(1), pp. 93–105.

[2] Volandri, G., Di Puccio, F., Forte, P., and Carmignani, C., 2011, "Biomechanics of the Tympanic Membrane," J. Biomech., **44**(7), pp. 1219–1236.

[3] Liang, J., Fu, B., Luo, H., Nakmali, D., Gan, R. Z., and Lu, H., 2015, "Characterisation of the Nonlinear Elastic Behaviour of Guinea Pig Tympanic Membrane Using Micro-Fringe Projection," Int. J. Exp. Comput. Biomech., **3**(4), pp. 319–344.

[4] Sharghi, H., Shakouri, M., and Kouchakzadeh, M. A., 2016, "An Analytical Approach for Buckling Analysis of Generally Laminated Conical Shells Under Axial Compression," Acta Mech., **227**(4), pp. 1181–1198.

[5] Dung, D. V., Hoa, L. K., Thuyet, B. T., and Nga, N. T., 2016, "Buckling Analysis of Functionally Graded Material (FGM) Sandwich Truncated Conical Shells Reinforced by FGM Stiffeners Filled Inside by Elastic Foundations," Appl. Math. Mech., **37**(7), pp. 879–902.

[6] Anh, V. T. T., and Duc, N. D., 2016, "The Nonlinear Stability of Axisymmetric Functionally Graded Material Annular Spherical Shells Under Thermo-Mechanical Load," Mech. Adv. Mater. Struct., **23**(12), pp. 1421–1429.

[7] Anh, V. T. T., Bich, D. H., and Duc, N. D., 2015, "Nonlinear Stability Analysis of Thin FGM Annular Spherical Shells on Elastic Foundations Under External Pressure and Thermal Loads," Eur. J. Mech. A, **50**, pp. 28–38.

[8] Duc, N. D., Anh, V. T. T., and Cong, P. H., 2014, "Nonlinear Axisymmetric Response of FGM Shallow Spherical Shells on Elastic Foundations Under Uniform External Pressure and Temperature," Eur. J. Mech. A, **45**, pp. 80–89.

[9] Sofiyev, A. H., and Kuruoglu, N., 2013, "Non-Linear Buckling of an FGM Truncated Conical Shell Surrounded by an Elastic Medium," Int. J. Pressure Vessels Piping, **107**, pp. 38–49.

[10] Manning, S. D., 1969, "General Instability of a Cylindrical Shell With Conical Ends Subject to Uniform External Pressure," Ph.D. thesis, Texas Technological College, Lubbock, TX.

[11] Baruch, M., and Singer, J., 1963, "General Instability of Stiffened Circular Conical Shell Under Hydrostatic Pressure," Technion Isroel Institute of Technology, Haifa, Israel, TAE Report No. 28.

[12] Steyer, C. C., and Zien, S.-C., 1961, "General Instability of an Orthotropic Circular Conical Shell Under Hydrostatic Pressure," Developments in Mechanics, 7th Midwestern Mechanics Conference, Michigan State University, East Lansing, MI, Sept. 6–8, Vol. I, pp. 153–176.

[13] Kendrick, S., 1953, "The Buckling Under External Pressure of Circular Cylindrical Shells With Evenly Spaced, Equal Strength, Circular Ring Frames—Parts I," Naval Construction Research Establishment, Dunfermline, UK, Report No. N.C.R.E./R211.

[14] Kendrick, S., 1953, "The Buckling Under External Pressure of Circular Cylindrical Shells With Evenly Spaced, Equal Strength, Circular Ring Frames—Parts II," Naval Construction Research Establishment, Dunfermline, UK, Report No. N.C.R.E./R243.

[15] Kendrick, S., 1953, "The Buckling Under External Pressure of Circular Cylindrical Shells With Evenly Spaced, Equal Strength, Circular Ring Frames—Parts III," Naval Construction Research Establishment, Dunfermline, UK, Report No. N.C.R.E./R244.

[16] Flügge, W., 1960, *Stresses in Shells*, Springer-Verlag, Berlin.